FishTaxa (2020) 16: 19-28
Journal homepage: www.fishtaxa.com

Descriptive osteology of *Garra rossica* (Nikolskii, 1900)

Maryam SAEMI-KOMSARI[1,2], Hamed MOUSAVI-SABET[1,2,*], Masoud SATTARI[1,2], Soheil EAGDERI[3], Saber VATANDOUST[4], Ignacio DOADRIO[5]

[1]*Department of Fisheries, Faculty of Natural Resources, University of Guilan, Sowmeh Sara, Iran.*
[2]*The Caspian Sea Basin Research Center, University of Guilan, Rasht, Iran*
[3]*Department of Fisheries, Faculty of Natural Resources, University of Tehran, Karaj, Iran.*
[4]*Department of Fisheries, Babol Branch, Islamic Azad University, Babol, Iran.*
[5]*National Museum of Natural Sciences, Spain*
*Corresponding author: *E-mail: mousavi-sabet@guilan.ac.ir*

Abstract

To describe the osteological structure of the *Garra rossica,* ten specimens were collected from the Mashkid Basin, Iran. After fixation into 10% buffered formalin, they were cleared and stained for osteological examination. Then its detailed osteological description was provided and compared with the available congeners in the genus *Garra* and other cyprinids. Based on the results, some differences have been found in different bones, including neurocranium, upper and lower jaws, pectoral and pelvic girdles, dorsal, anal and caudal fins skeleton, and circumorbital series.

Keywords: Skeleton, *Garra*, Cyprinidae, Lotak, Iran.
Zoobank: urn:lsid:zoobank.org:pub:C54BB8A3-EE04-4BC6-A98D-DFA2BC1DDCD2

How to cite: Saemi-Komsari M., Mousavi-Sabet H., Sattari M., Eagderi S., Vatandoust S., Doadrio I. 2020. Descriptive osteology of *Garra rossica* (Nikolskii, 1900). FishTaxa 16: 19-38.

Introduction

The genus *Garra* Hamilton, 1822 with about 170 valid species is one of the most diverse genera of the family Cyprinidae, which are widely distributed in tropical and subtropical Asia, Africa and the Middle East (Menon 1964; Yang and Mayden 2010; Sayyadzadeh et al. 2015; Mousavi-Sabet and Eagderi 2016; Vatandoust et al., 2019). The genus *Garra* consist of 14 valid species in Iranian inland waters distinguishing by some morphological characters, especially mouth form and dorsal fin rays (Esmaeili et al. 2018; Çiçek et al. 2018; Mousavi-Sabet et al., 2019), as well as the absence of scales and eyes in those subterranean species. Some *Garra* species have been recently described from Iran, including *G. mondica* (Sayyadzadeh et al. 2015), *G. lorestanensis* (Mousavi-Sabet and Eagderi 2016), *G. tashanensis* (Mousavi-Sabet et al. 2016), *G. amirhosseini* (Esmaeili et al. 2016) and *G. roseae* (Mousavi-Sabet et al. 2019).

Osteological characters can provide valuable information for various purposes such as phylogenetic analysis (Diogo and Bills 2006; Azimi et al. 2015; Nasri et al. 2016), archaeology (Carnevale et al. 2011; Hilton 2003), and ontogeny and developmental studies (Britz 1996; Britz and Conway 2009; Fiaz et al. 2012) of fishes. In the genus *Garra*, due to a few morphological distinguishable characters in terms of taxonomy, osteological characters can be useful for providing further distinguishig characters. Although some biological aspects of some *Garra* species have been investigated, so far, no detailed study has been made on the osteology of *G. rossica*. In addition, sme works have been done on the osteology of other species of this genus, including *G. typhlops* (Jalili and Eagderi 2014), *G. persica,* and *G. ruffa* (Esmaeilzadegan 2013; Zamani-Faradonbe and Keyvani 2018). In this regard, this work was conducted to provide a detailed descriptive osteology of *G. rossica* that can help for better understanding of its taxonomic status and provide further information for taxonomic and phylogenic relationships of the genus *Garra* as well.

Material and Methods

Ten specimens of *G. rossica* (32.8-52.7 in standard length) were collected from the Nahang River, Mashkid basin, Iran (26°50'36.1"N 61°35'27.7"E) using an electro-fishing device. After anesthesia in 1% clove-oil

Accepted: 22 January 2020; Published: 9 July 2020

Figure 1. Lateral view of skeletal structure of *Garra rossica* from the Nahang River, Iran (scale bar = 5 mm).

solution, the specimens were fixed into 10% buffered formaldehyde. Then, the specimens were cleared and stained using alizarin red S and alcian blue for the osteological examination (Taylor 1967) (Fig. 1). Images of the stained skeletal structures were captured by scanner (Epson V600) using glycerol bath. Skeletal structures were examined by stereomicroscope (Leica M5). The skeletal elements were drawn based on 2D digital pictures using CorelDraw X7 software. The skeletal nomenclatures follow Howes (1982) and Rojo (1991).

Results

The neurocranium was almost rectangular in shape with extensions, including two lateral ethmoid and two sphenoid processes (Fig. 2a). The supraethmoid-ethmoid, lateral ethmoid, pre-ethmoid and vomer are the components of ethmoid region. The ethmo-vomerine region is laterally concaved; three grooves are appeared on its anterior margin (shown in circle Fig. 2b). The small pre-ethmoid situates in the antero-lateral edge of the vomer distinguished with semicircular shape. The vomer is posteriorly linked to the parasphenoid and lateral-ethmoid (Fig. 2a, c).

The orbital region consists of the frontal, orbitosphenoid, pterspheno id, parasphenoid and circumorbital elements (Fig. 2a, b, c). The frontal is medially wide and its ventro-medial edge is connected to the orbitosphenoid and pterspheno id (Fig. 2a, b). The parasphenoid is wider in the middle part (Fig. 2a). The two orbitosphenoids are connected to the parasphenoid ventrally (Fig. 2a, c). The parasphenoid is extended from the basioccipital to vomer connected ventrally to the neurocranium. The ventro-lateral expansion of the parasphenoid in the middle part is place for ligamentous connection of the pharyngobranchials (Fig. 2a). The circumorbital series consists of five infra-orbitals (Fig. 2d) that the first one is triangular lachrymal bone that beara a pointed process. The 2nd element is elongated, and its anterior part is wider and 3rd one is elongated and internally concaved (Fig. 2d). In addition, this series are consisted of a paired supra-orbital element laterally connected to the frontal (Fig. 2b). The supraorbital is elliptic-shaped, and its positions beside the frontal and lateral process of lateral ethmoid (Fig. 2b).

The otic region consists of the parietal, epiotic, sphenotic, pterotic, dermopterotic and prootic. The parietal is asymmetrical in shape and the sphenotic and supraoccipital situate in dorso-lateral and postero-dorsal sides of the neurocranium, respectively (Fig. 2b, c). The sphenotic bears a lateral process and ventrally attached to the prootic and postero-dorsally to the pterotic (Fig. 2a, b). The epiotic occupies the space between the pterotic and supraoccipital (Fig. 2b).

The occipital region consists of the supraoccipital, exoccipitals and basioccipital (Fig. 2a, b). The supraoccipital postero-laterally attached to the epiotic (Fig. 2b). The exoccipital distinguished bay having ventral foramen and its middle portion is concaved (Fig. 2a, c). The anterior margin of the basioccipital is ventrally and dorsally connected to the prootic and parasphenoid (Fig. 2a, c). The basioccipital includes a posterior pharyngeal

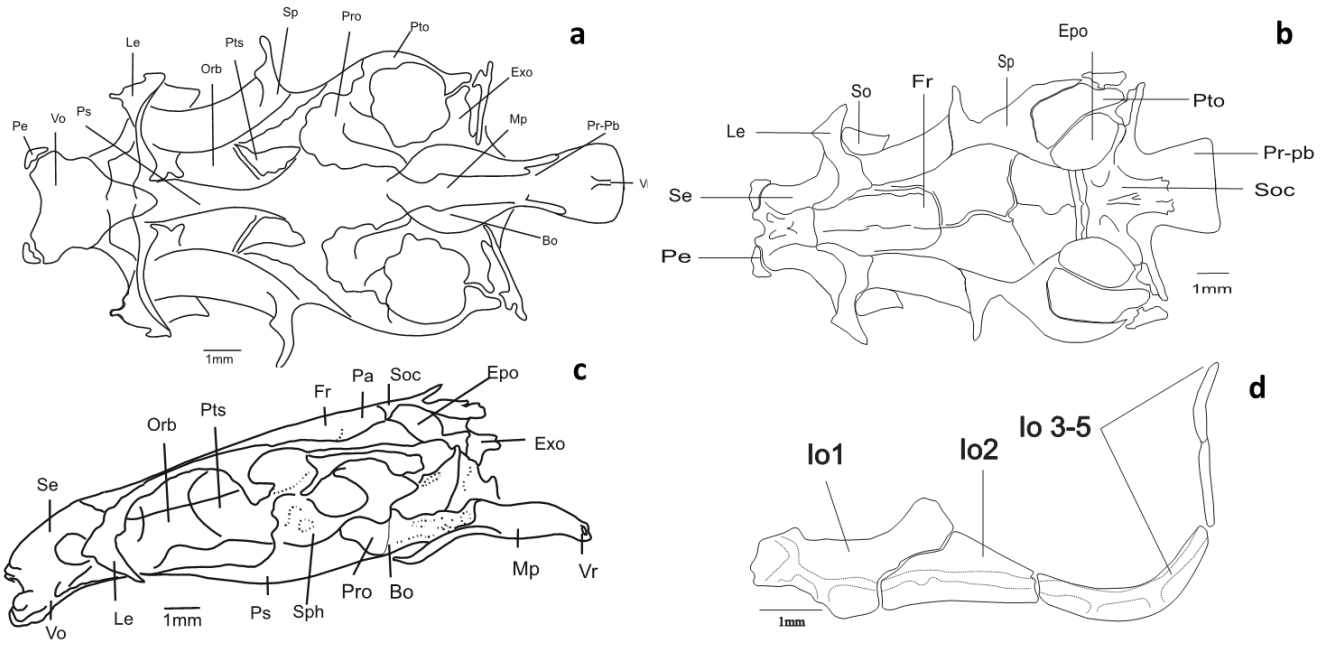

Figure 2. Neurocranium of *Garra rossica* in (a) ventral, (b) dorsal and (c) lateral views, and (d) circumorbital series. Abbreviations: Bo: basioccipital; Epo: epiotic; Exo: exoccipital; Fr: frontal; Le: lateral ethmoid; Mp: ventral masticatory plate; Orb: orbitosphenoid; Pa: parietal; Pe: preethmoid I; Pro: prootic; pr-Pp: posterior pharyngeal process; Ps: parasphenoid; Pto: pterotic; Pts: pterosphenoid; Se: supraethmoid; Soc: supraoccipital; so: msupraorbital; Sp: sphenotic; Vo: vomer; So: Supraorbital; Vr: ventromedial ridge. And in lateral view of circumorbital series: Io-1-6 - Infraorbital 1-6; IO1-Infra orbital1 (lachrymal); IO2-Infra orbital2 (Jugal) (scale bar = 1 mm).

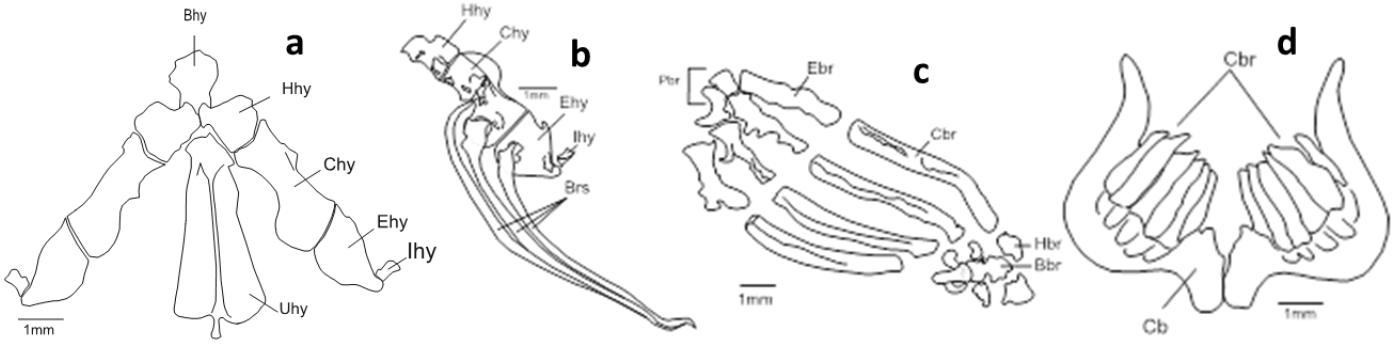

Figure 3. *Garra rossica*: (a) dorsal and (b) lateral view of the hyoid arches, (c) branchial apparatus and (d) pharyngeal teeth. Abbreviations: Bhy: basihyal; Chy: ceratohyal; Epi: epihyal; Hhy: dorsal and ventral hypohyal; Ihy: interhyal; Uhy: urohyal; Bbr: basibranchial; Cbr: Ceratobranchial rakers (Pharyngeal teeth); Ebr: epibranchial; Hbr: hypobranchial; Pbr: pharyngobranchial (scale bar = 1 mm).

process and a ventral masticatory plate (Fig. 2a). Two antero-lateral processes of the masticatory plate are small and its anterior rim bended dorsally (Fig. 2a). The posterior pharyngeal process has a dorsal fossa and a ventromedial ridge (Fig. 2a, b).

The hyoid arch consists of the unpaired basihyal and urohyal and paired epihyals, dorsal and ventral hypohyals, ceratohyals and three pairs of branchiostegal rays (Fig. 3a, b). The small basihyal is the anterior most element of the hyoid arch (Fig. 3a, b) that dorsally is wider than its ventral part. The largest element of the hyoid arch is urohyal having a blade-shape vertical element in its dorsal side and possessing a protruded process posteriorly (Fig. 3a). There is a V-shaped notch on the posterior edge of the horizontal part of the urohyal (Fig. 3a). Three branchiostegals, one hypohyal, one ceratohyal, one epihyal and one interhyal form each half of the hyoid arch. The two hypohyals positioned on both upper sides of the urohyal creating junction for the basihyal. The two internal branchiostegals are connected to the ceratohyal and the last ones are connected to the epihyal

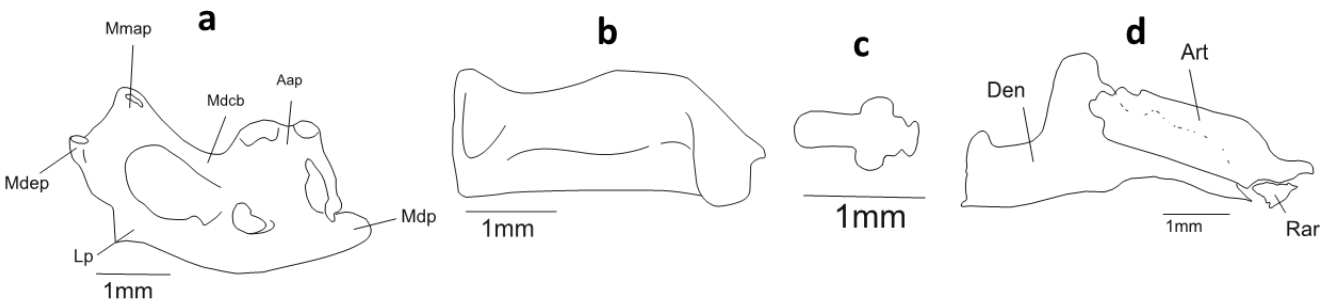

Figure 4. *Garra rossica*: Medial view of upper jaw (a) maxilla, (b) premaxilla, (c) kinethmoid, and (d) medial view of lower jaw. Abbreviations: Art: articular; Den: dentary; Rar: retroarticular Lp: lateral process; Aap – Anterior ascending process; Mdcb – maxillary dorsal concaved border; Mdep – maxillary descending process; Mdp – maxillary distal process; Mmap – maxillary mid lateral ascending process (scale bar = 1 mm).

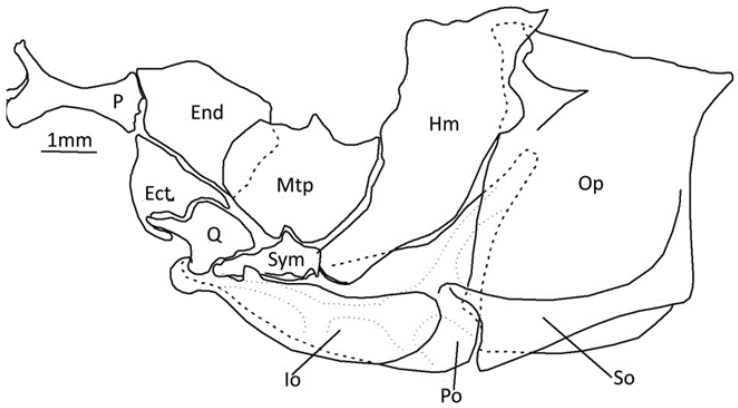

Figure 5. *Garra rossica*: Lateral view of the suspensorium and opercular series. Abbreviations: Ect: ectopterygoid; End: endopterygoid; Hm: hyomandibular; Io: interopercle; Mtp: metapterygoid; Op: opercle; P: palatine; Po: preopercle; Q: quadrate; So: subopercle; Sym: symplectic (scale bar = 1 mm).

by connective tissue. The hypohyal ventrally has a relatively large cavity with a large articulatory facet to articulate the urohyal (Fig. 3b). The middle part of the ceratohyal is narrower, and its ventral margin is concaved. The epihyal is slightly triangular in shape and possesses a light posterior process dorsally bended (Fig. 3a, b).

The upper jaw comprises the paired premaxilla, maxillae and kinethmoid (Fig. 4a, b, c). The middle part of the maxillae is curved and its anterior side is wider. The shape of this bone from anterior to posterior includes that anterior ascending process, concaved dorsal part, a descending process, a distal process, a mid-lateral ascending process, lateral process, and foramen (Fig. 4a). The kinethmoid is situated between the two maxillae, that its middle portion has two lateral processes (Fig. 4c). The maxilla is larger than premaxilla in size, and its dorsal border is concaved between the maxillary mid-lateral ascending and anterior ascending processes. The mid-lateral ascending process of the maxillae is positioned near its distal part. The lower jaw included the dentary, articular and retroarticular (Fig. 4d). The dentary as the biggest bone in is curved and medially showed protuberances (Fig. 4d). The articular is narrow in its anterior part and overlapped with the posterior part of the dentary. The triangular-shaped retroarticular is small and positioned postero-ventrally to the articular. The posterior articulatory facet of the lower jaw is formed by the articular and retroarticular bones.

The suspensorium composes of seven bones, including the palatine, endopterygoid, ectopterygoid, quadrate, symplectic, metapterygoid and hyomandibular (Fig. 5). The hyomandibular is articulated the suspensorium to the neurocranium. The anterior part of the palatine is larger with extending three branched process articulating to the preethmoid. The endopterygoid postero-dorsally is connected to the upper edge of the palatine. The ectopterygoid has triangle shape as its two angle antero-ventrally beside the quadrate have processes inwardly inclined and cover the quadrate and laterally connected to the endopterygoid. The symplectic is medially attached to the quadrate that covers the symplectic ventrally. The metapterygoid is positioned anteriorly, ventrally and posteriorly between the endopterygoid, quadrate and symplectic, respectively and is connected to

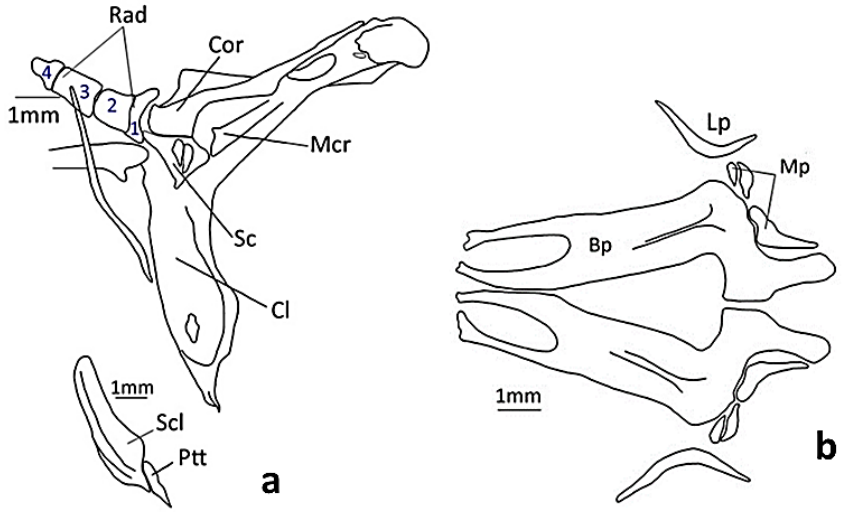

Figure 6. *Garra rossica*: (a) Internal view of the pectoral girdle, and (b) ventral view of the pelvic girdle. Abbreviations: Bp: Basipterygium; Cl: cleithrum; Cor: coracoid; Lp: lateral pterygium; Mcr: mesocoracoid; Mp: metapterygium; Ptt: posttemporale; Rad: ossified pectoral radial; Sc: scapula; Scl: supracleithrum (scale bar = 1 mm).

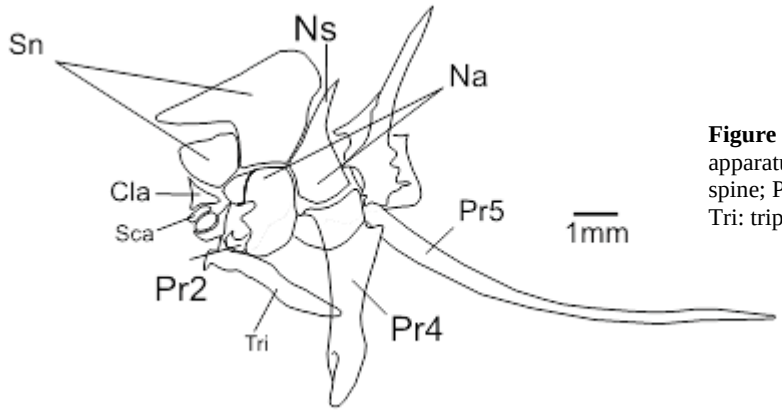

Figure 7. *Garra rossica*: lateral view of the Weberian apparatus. Abbreviations: Na: neural arch; Ns: neural spine; Pr: pleural rib; Sn: supraneural. Sca: scaphium; Tri: tripus; Int: intercalarium (scale bar = 1 mm).

the hyomandibular by connective tissue.

The branchial apparatus composes of the two unpaired basibranchial, three paired hypobranchials, four paired ceratobranchial, four paired epibranchial and two paired pharyngobranchial bones (Fig. 3c). In *G. rossica*, there are three rows of the pharyngeal teeth with a dental formula of 3.5.6-6.5.3 (Fig. 3d).

The opercular series consist of the preopercle, opercle, subopercle and interopercle (Fig. 5). The two arms of the preopercle form a right angle to each other. The posterior and ventral border of the preopercle covers the three other opercular bones. The opercle is the largest element of this series, and along with the subopercle are connected to the head of the interopercle by connective tissue. The interopercle is positioned under the preopercle and connected to the lower jaw by connective tissue.

The pectoral girdle includes the cleithrum, supracleithrum, coracoid, mesocoracoid, scapula, posttemporal and radials (Fig. 6a). The ventral part of the cleithrum is wider with a lateral process and became narrower with a pointed process posteriorly (Figs. 6a). The supracleithrum is positioned on the dorsal side of the cleithrum. The posttemporal is a small bone that connects the pectoral girdle to the pterotic. The coracoid is attached to the long mesocoracoid that is connected the coracoid to the cleithrum. The scapula is surrounded between the coracoid and cleithrum. The two large foramen are observed in the middle part of the coracoid. The pectoral girdle of *G. rossica* bears four radials and the first one is positioned in the furthest distance from the pectoral girdle, is the smallest one, and the third one is the largest. The thickest radial is fourth one connected to the scapula and coracoid (Fig. 6a). The first unbranched pectoral fin ray is directly connected to the scapula, but

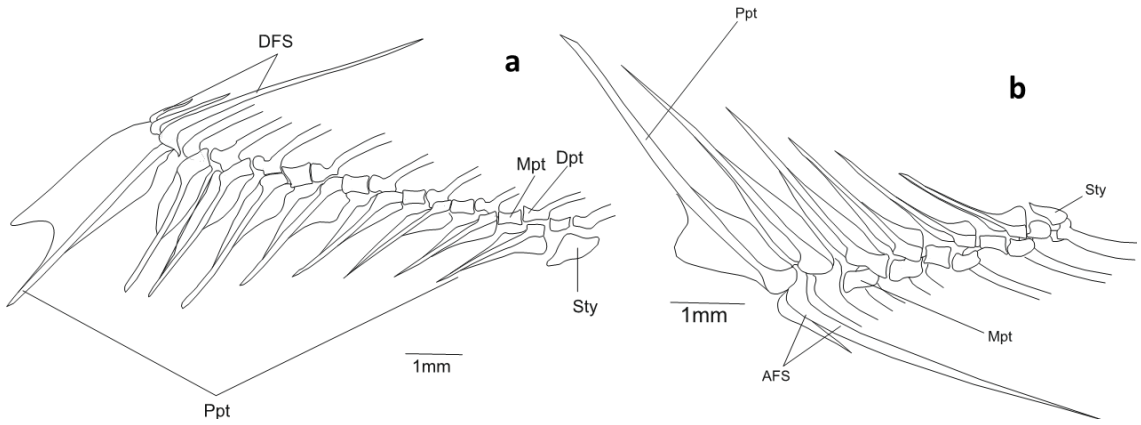

Figure 8. *Garra rossica*: Dorsal (a) and anal fins (b) skeleton (AFS- Anal Fin Spine; DFS- Dorsal Fin Spine; Dpt- Distal Petrigiophore; MPt- Median Petrigiophore; PPt- Proximal Pterigiophore; Sty- Stay) (scale bar = 1 mm).

others connected to the pectoral girdle mediated by radials.

The basipterygium, three metapterygium (actinosts) and lateral pterygium presents in each side of the pelvic fin. The posterior part of the basipterygium is wider with a process inclined backwardly, and its anterior part is bifurcated by a deep hollow. In *G. rossica,* the two arms are equal in size and internal one is a bit curved in to the external one. Three paired of the metapterygium are located medially near the basipterygium; the internal metapterygium (actinosts) in each side is the largest one. A paired lateral pterygium (actinosts) was laterally positioned beside the basipterygium (Fig. 6b).

Weberian apparatus includes the claustrum, scaphium, intercalarium and tripus (Fig. 7). The tripus is positioned on the second vertebrae and its posterior part passes underneath of the third vertebrae ribs. The first centrum with two lateral processes is deformed and thinned, and its ribs are absent. The pleural rib of the second centrum backwardly bended, and the pleural rib of the fourth centrum is wide with a latero-internal process (Fig. 7). The supernatural and neural arches are originated from the first and second centrum (Fig. 7). The first two supraneurals (neural complex) are connected to their related vertebrae. The second supraneural as the largest one. In the axial skeleton, vertebral number is 29. The ventral and caudal parts of the vertebral column have 15 and 14 vertebrae, respectively (Fig. 1).

The dorsal fin includes three unbranched fin rays, nine proximal pterigiophore, nine median pterygiophores, and one stay (Fig. 8a). Three elements of the pterygiophore include distal, medial and proximal processes. The first proximal in pterygiophore is the largest one that supports three unbranched rays (Fig. 8a). The anal fin has two unbranched rays and six branched rays, six pterygiophores and one stay bone. The largest pterygiophore supports two unbranched rays (Fig. 8b).

The caudal fin includes six hypurals, epural, parhypural, pleurostyle, uroneural bones. The caudal fin supports 29 branched rays. Neural spine of the second centrum has changed into a small pointed process. The two uroneural ossicles are situated in both sides of the eurostyle and are the same size and shorter than the hypural 6 (Fig. 9). The epural is posteriorly extended from the neural process (rNP).

Discussion

In the neurocranium of *G. rossica*, the lateral ethmoid with less depth is different in shape with that of *G. typhlops* (Esmaeilzadegan 2013). In addition, there are five infra-orbital bones in *G. rossica*, however no lachrymal and infra-orbital bones are found *G. typhlops*. The supraethmoid of *G. rossica* is elongated posteriorly connecting to the lateral process of the preethmoid and there is no ethmoid similar to *Alburnus sellal* (Jalili et

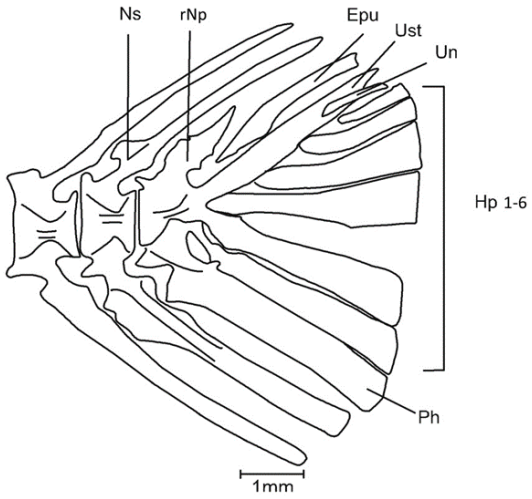

Figure 9. *Garra rossica*: Left lateral view of the caudal skeleton in Garra rossica. Elaborations: Epu: epural; Hp: hypurals; rNp: rudimentary neural process; Ns: neural spine; Ph: parhypurale; Un: uroneural; Ust: urostile (scale bar = 1 mm).

al. 2015). However, the ethmoid is found in *Cyprinion milesi* (Nasri et al. 2016). Despite *G. rossica*, in some cyprinids such as *Squalius* and *Scardinius*, the preethmoid is absent (Ramaswami 1995).

The vomer of *G. rossica* is posteriorly overlapped by the parasphenoid; however, the prevomer of *C. milesi* is posteriorly overlapped by the parasphenoid similar to those of *Schizothorax* and *Orienus* (Ramaswami 1995; Nasri et al. 2016). The shape of the vomer varies in cyprinid fishes; in some fishes, it is blunt and non-pointed, but in some others is elongated and pointed (Ramaswami 1995). The posterior edge of the vomer was rounded in *G. rossica* with its anterior rim same as *G. typhlops* (Jalili and Eagderi 2014); while, its anterior rim positioned beneath the supraethmoid as same as *G. rufa,* but in difference position with *G. typhlops* i.e. it positions anterior to the supraethmoid-ethmoid complex. Moreover, the rim of the vomer showed little difference between *G. rossica* and *G. persica*, whereas the differences are remarkable compared to *G. typhlops* (Esmaeilzadegan 2013; Jalili and Eagderi 2014; Zamani-Faradonbe and Keivany 2018). The anterior part of the parasphenoid is narrower with a small notch on its anterior rim in *G. rossica* similar to *G. rufa* and *G. persica* (Esmaeilzadegan 2013; Zamani-Faradonbe and Keivany 2018), whereas it is wider than its posterior part with a deep groove in *Disgobio* and *Discocheilus,* and *G. typhlops* (Zhang 2005; Jalili and Eagdari 2014). *Garra rossica* despite *G. persica* (Zamani-Faradonbe and Keivany 2018) as more expanded spehenotic part, parietal and rudimentary development of the frontal. In addition, the supraorbital of *G. rossica* is elliptic-shaped and positioned beside the frontal and lateral process of the lateral ethmoid as same as *C. milesi,* and *G. persica* (Nasri et al. 2016; Zamani-Faradonbe and Keivany 2018), whereas it was reduced in *G. typhlops* (Jalili and Eagdari 2014).

In *G. rossica*, the notch of the dorsal margin in the lateral portion of maxillary (Mmap, Mdep) has shorter length than *G. typhlops* (Jalili and Eagdari 2014) but is similar to *G. persica, G. typhlops*, *C. macrostomum* and *C. kais* (Nasri et al. 2013; Jalili and Eagdari 2014; Zamani-Faradonbe and Keivany 2018), *C. mhalensis* and *C. acinaces* (Alkahem et al. 1990). The anterior ascending process of the maxilla in *G. rossica* is shallow and thick similar to *C. milesi* and other cyprinids (Howes 1982; Nasri et al. 2013, 2016). The lateral process of the maxilla is small and reduced in *G. rossica* the same as *G. typhlops* (Jalili and Eagdari 2014) but it is well-developed in *C. milesi* (Nasri et al. 2016).

In the lower jaws of *G. rossica* like *G. typhlops*, the articular and retroarticular contribute to form the articulatory facet of the dentary, whereas in the *G. rufa* only articular forms this facet (Esmaeilzadegan 2013). Differences in the lower jaws is led to variation of the mouth shape (Nasri et al. 2016). In addition, the masticatory plate of *G. rossica* is larger than that of *G. typhlops.* Therefor all these differences could be related to adaptation to their different inhabitant environment and feeding habits and behavior. These fishes live in dry

and unstable habitats, therefore; they are adapted to massive changes in water level, temperature and oxygen content as well as availability of food (Krupp 1988, 2009). Smaller size of the masticatory plate in *G. typhlops* comparing with *G. rossica* could refer to its detritivore behavior (Sargeran et al. 2008) and therefore, may not need a larger and strong one as seen in *G. persica,* and *G. rossica*. The suspensorium elements, especially the ectopterygoid and endopterygoid in *G. rossica* are not as expanded as *G. typhlops*. This feature shows shorter length of the head in *G. rossica* comparing with *G. typhlops* while they are the same as *G. persica*.

In the pelvic girdle of *G. rossica*, number of the metapterygium was different with that of *G. persica* (one pair metapterygium) (Zamani-Faradonbe and Keivany 2018) and has same number with *G. typhlops* (Jalili and Eagdari 2014). Moreover, the ossified pectoral radial bones of the pectoral girdle in *G. rossica* and *G. typhlops* are equal in number (n=4) vs. three in *G. persica.* The stoutness of the neural spins in the genera *Cyprinion* and *Garra* has been denoted in Arabian Peninsula (Alkahem et al. 1990). The second supraneural as the largest one is trapezoid shape in *G. rossica* vs. t-shape in *C. kais.*

In the axial skeleton, vertebral number is 29 which are the same numbers comparing with *G. typhlops* and *G. persica.* The ventral and caudal parts of the vertebral columnhave 15 and 14 vertebrae, respectively. However, comparing the proportion of the centra number in the ventral and caudal of in *G. typhlops* and *G. rossica* showed almost the same trend vs. less number of the ventral centra (n=12) in *G. persica*. It is supposed that ventral cavity in *G. persica* should be bigger than *G. rossica* and *G. typhlops*. Instead of that longer caudal part in *G. rossica* and *G. typhlops* could be related to the adaptation to their inhabitants which need to have better swimming and maneuver in water flows.

Dorsal fin skeleton in *G. rossica* and *G. typhlops* showed more similarity than that of *G. persica* which showed differences in the number unbranched rays (n=2-3 in *G. persica* vs. n=3 in *G. rossica* and *G. typhlops*) and dorsal rays (branched rays) (n=9 vs. 10). Anal fin of *G. rossica* and *G. typhlops* (Jalili and Eagderi 2014) showed the two unbranched rays comparing with the one unbranched ray in *G. persica* (Zamani-Faradonbe and Keivany 2018). However, the number of petrigiophores in *G. typhlops* (n=7) was different from *G. rossica* and *G. persica* (n=6). There is a distinguishable difference in the structure of the neural spine of *G. rossica* than *G. persica* and *G. rossica* in shape.

In conclusion, our study identified some differences in the shape, structure, and number of bony elements in *G. rossica* compared to previous studies on the other species of the genus *Garra* which can be related to their biological traits, life history considering adaptation to their inhabitants

Acknowledgements

The authors would like to thank Ms. P. Jalili for her assistant during the laboratory work.

Literature cited

Alkahem H.F., Behnke R.J. Ahmad Z. 1990. Some osteological distinction among four Arabian cyprinid species Japanese Journal of Ichthyology 36: 477-482.

Azimi H., Mousavi-Sabet H., Eagderi S., Vatandoust S. 2015. Osteological characteristics of Turkmenian stone loach, *Paraschistura cristata* (Cypriniformes: Nemacheilidae). International Journal of Aquatic Biology 3(5): 290-300.

Britz R. 1996. Ontogeny of the ethmoidal region and hyopalatine arch in *Macrognathus pancalus* (Percomorpha, Mastacembeloidei), with critical remarks on Mastacembeloid inter and intrarelationships. American Museum Novitates 3181: 1-18.

Britz R., Conway K.W. 2009. Osteology of *Paedocypris*, a miniature and highly developmentally truncated fish (Teleostei: Ostariophysi: Cyprinidae). Journal of Morphology 270: 389-412.

Carnevale G., Haghfarshi E., Abbasi S., Alimohammadian H., Reichenbacher B. 2011. A new species of silverside from

the Late Miocene of NW Iran. Acta Palaeontologica Polonica 56(4): 749-756

Çiçek E., Fricke R., Sungur S., Eagderi S. 2018. Endemic freshwater fishes of Turkey. FishTaxa 3(4): 1-39.

Diogo R., Bills R. 2006. Osteology and myology of the cephalic region and pectoral girdle of the South African catfish *Austroglanis gilli*, with comments on the autapomorphies and phylogenetic relationships of the Austroglanididae (Teleostei: Siluriformes). Animal Biology 56(1): 39-62.

Esmaeili H.R., Sayyadzadeh G., Coad B.W., Eagderi S. 2016. Review of the genus *Garra* Hamilton, 1822 in Iran with description of a new species: a morpho-molecular approach (Teleostei: Cyprinidae). Iranian Journal of Ichthyology 3(2): 82-121.

Esmaeili H.R., Sayyadzadeh G., Eagderi S., Abbasi K. 2018. Checklist of freshwater fishes of Iran. FishTaxa 3(3): 1-95.

Esmaeilzadegan E. 2013. Comparison of morphological characteristics of the sang-lis (*Garra ruffa*) and Iranian cave fish (*Iranocypris typhlops*). M.Sc. thesis, Department of Fisheries, University of Tehran. 71 p. (In Persian)

Fiaz A.W., Léon-Kloosterziel K.M., Gort G., Schulte-Merker S., van Leeuwen J.L., Kranenbarg S. 2012. Swim-training changes the spatio-temporal dynamics of skeletogenesis in zebrafish larvae (*Danio rerio*). PLoS ONE 7(4): e34072.

Hilton E.J. 2003. Comparative osteology and phylogenetic systematics of fossil and living bony-tongue fishes (Actinopterygii, Teleostei, Osteoglossomorpha). Zoological Journal of the Linnean Society 137(1): 1-100.

Howes G.J. 1982. Anatomy and evolution of the jaws in the semiplotine carps with a review of the genus *Cyprinion* Heckel, 1843 (Teleostei: Cyprinidae). Bulletin of the British Museum (Natural History), Zoology 42(4): 299-335.

Jalili P., Eagderi S. 2014. Osteological description of Iran cave barb (*Iranocypris typhlops* Bruun & Kaiser, 1944). University Journal of Zoology, Rajshahi University 33: 01-07.

Jalili P., Eagderi S., Azimi H., Mousavi-Sabet H. 2015. Osteological description of the southern king fish, *Alburnus mossulensis* from Iranian part of the Tigris River drainage. ABAH Bioflux 7(2): 113-121.

Kafuku T. 1969. Morphological differentiation of *Cyprinion* in Iraq. Bulletin of freshwater fisheries research laboratory 19: 155-160.

Krupp F. 1988. Freshwater fishes of the Wadi Batha drainage. Journal of Oman Studies 401–404

Krupp F., Budd K. 2009. A new species of the genus *Garra* (Teleostei: Cyprinidae) from Oman. Aqua 15(2):117-120

Menon A. 1964. Monograph of the cyprinid fishes of the genus *Garra* Hamilton. Mem Indian Museum 14:173-260

Mousavi-Sabet H., Eagderi S. 2016. *Garra lorestanensis*, a new cave fish from the Tigris River drainage with remarks on the subterranean fishes in Iran (Teleostei: Cyprinidae). FishTaxa 1:45-54.

Mousavi-Sabet H., Vatandoust S., Fatemi Y., Eagderi S. 2016. Tashan cave a new cave fish locality for Iran; and *Garra tashanensis*, a new blind species from the Tigris River drainage (Teleostei: Cyprinidae). FishTaxa 1(3):133-148.

Mousavi-Sabet H., Saemi-Komsari M., Doadrio I., Freyhof J. 2019. *Garra roseae*, a new species from the Makran region in southern Iran (Teleostei: Cyprinidae). Zootaxa 4671: 223-239.

Nasri M., Eagderi S., Farahmand H., Hashemzade-Segherloo I. 2013. Body shape comparison of *Cyprinion macrostomum* (Heckel, 1843) and Cyprinion watsoni (Day, 1872) using geometric moprphometric method. International Journal of Aquatic Biology 1: 240-244.

Nasri M., Eagderi S., Farahmand H. 2016. Descriptive and comparative osteology of Bighead Lotak, *Cyprinion milesi* (Cyprinidae: Cypriniformes) from southeastern Iran. Vertebrate Zoology 66(3): 251-260.

Ramaswami L.S. 1995. Skeleton of Cyprinoid fishes in relation to phylogenetic studies: 6. The skull and weberian apparatus of Cyprininae (Cyprinidae). Acta Zoologica 36: 199-242.

Rojo A.L. 1991. Dictionary of Evolutionary Fish Osteology: CRC Press. 282 p.

Sargeran P., Bakhtiyari M., Abdoli A., Coad B.W., Sarvi K., Rahmati Lishi M., Hajimoradloo A. 2008. The endemic Iranian Cave-fish, Iranocypris typhlops: two taxa or two forms based on the mental disc? Zoology in the Middle East 44: 67-74.

Sayyadzadeh G., Esmaeili H.R., Freyhof J. 2015. *Garra mondica*, a new species from the Mond River drainage with remarks

on the genus Garra from the Persian Gulf basin in Iran (Teleostei: Cyprinidae). Zootaxa 4048: 075-089.

Taylor W. R. 1967. An enzyme method of clearing and staining small vertebrates. Proceedings of the United States National Museum 122: 1-17.

Vatandoust S., Mousavi-Sabet M., Geiger M.F., Freyhof J. 2018. A new record of Iranian subterranean fishes reveals the potential presence of a large freshwater aquifer in the Zagros Mountains. Journal of Applied Ichthyology 35(6): 1269-1275.

Yang L., Mayden R.L. 2010. Phylogenetic relationships, subdivision, and biogeography of the cyprinid tribe Labeonini (sensu Rainboth, 1991) (Teleostei: Cypriniformes), with comments on the implications of lips and associated structures in the labeonin classification. Molecular Phylogenetics and Evolution 54: 254-265

Zamani-Faradonbe M., Keivany Y. 2018. Descriptive osteology of Persian stone lapper (*Garra persica*) from Sistan basin. Journal of Animal Researches 30(3): 346-357.

Zhang E. 2005. Phylogenetic Relationships of Labeonine Cyprinids of the Disc-Bearing Group (Pisces: Teleostei). Zoological Studies 44: 130-143.